

Current Correlations in a Quantum Dot Ring: A Role of Quantum Interference

Bogdan R. Bułka and Jakub Łuczak

*Institute of Molecular Physics, Polish Academy of Sciences,
ul. M. Smoluchowskiego 17, 60-179 Poznań, Poland*

(Dated: April 30, 2022)

We present studies of electron transport and circular currents, those induced by the bias voltage and the magnetic flux threaded a ring of three quantum dots coupled with two electrodes. Quantum interference of electron waves passing through the states with opposite chirality play a relevant role in transport, one can observe the Fano resonance with destructive interference. The quantum interference effect is quantitatively described by local bond currents and their correlation functions. Fluctuations of the transport current are characterized Lesovik's formula for the shot noise, which is a composition of the bond current correlation functions. In the presence of circular currents the cross-correlation of the bond currents can be very large, but it is negative and compensates large positive auto-correlation functions.

PACS numbers: 72.10.-d; 73.23.b; 73.63.b; 73.21.La

I. INTRODUCTION

In 1985, Webb et al.¹ presented their pioneering experiment showing Aharonov-Bohm oscillations in a nanoscopic metallic ring and a role of quantum interference (QI) in electron transport. Later, Ji et al.² demonstrated the electronic analogue of the optical Mach-Zehnder interferometer (MZI), which was based on closed geometry transport through single edge states in the quantum Hall regime. Theoretical studies³⁻⁷ predicted coherent transport through single molecules with a ring structure, where due to their small size one could show constructive or destructive quantum interference effects at room temperatures. Since 2011 these predictions were experimentally verified using mechanically controllable break junction (MCBJ) and scanning tunneling microscope break junction (STM-BJ) techniques^{8,9} in various molecular systems: single phenyl, polycyclic aromatic, conjugated heterocyclic blocks as well as hydrocarbons (for a recent review on QI in molecular junctions see^{10,11} and references therein).

Our interest is in internal local currents and their correlations in a ring geometry to see a role of quantum interference. An interesting aspect is formation of a quantum vortex flow driven by a net current from a source to drain electrode, which was studied in many molecular systems^{7,10,12-21} (see also²²). It was also shown that under some conditions a circular thermoelectric current can exceed the transport current²³. In particular, our studies focus on a role the states with opposite chirality in the ring on the QI effect and the circular current. Correlations of the electron currents (shot noise) through edge states in the Mach-Zehnder interferometer were extensively studied by Buttiker and coworkers²⁴⁻²⁸ (see also²⁹ and references therein). However, in the metallic (or molecular) ring the situation is different than in MZI, because multiple reflections are relevant for formation of the circular current. Our studies will show that the transition from the laminar to the vortex flow is manifested in the shot noise of local currents. In particular, it will be

well seen in a cross-correlation function for the currents in different branches of the ring, which becomes negative and large in the presence of the circular current.

The paper is organized as follows. In the next chapter II we will present the model of the three quantum dots in the ring geometry, which is the simplest model showing all aspects of QI and current correlations. The model includes the magnetic flux threaded the ring, which changes interference conditions as well as induces a persistent current. The net transport current, the local bond currents as well as the persistent current (and their conductances) are derived analytically by means of the nonequilibrium Keldysh Green function technique. It will be shown that the correlation function for the net transport current can be expressed as a composition of the correlation functions for the local currents inside the ring. We will also show all shot noise components, in particular that one for the net transport current (given by Lesovik's formula³⁰). The next chapters III, IV and V present the analyze of the results for the case $\Phi = 0$ (without the magnetic flux), for the case with the persistent current only (without the source-drain bias V) and the general case (for $V \neq 0$, $\Phi \neq 0$) showing an interplay between the bond currents and the persistent current. The final section VI summarized the main results of the paper.

II. CALCULATIONS OF CURRENTS AND THEIR CORRELATIONS IN TRIANGULAR QUANTUM DOT SYSTEM

A. Model

The considered system of three quantum dots in an triangular arrangement is presented in Fig.1. The system is described by the Hamiltonian

$$H_{tot} = H_{3QD} + H_{el} + H_{3QD-el}, \quad (1)$$

which consists the parts corresponding to electrons in the triangular QD system, in the electrodes and the coupling

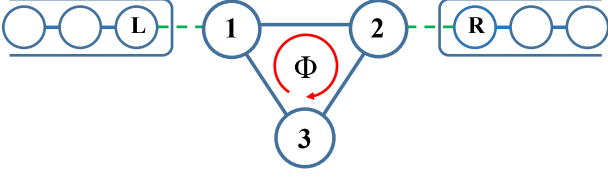


FIG. 1: Model of the triangular system of three quantum dots (3QDs) threaded by the magnetic flux Φ and attached to the left (L) and the right (R) electrode.

between the subsystems, respectively.

$$H_{3QD} = \sum_{i \in 3QD} \varepsilon_i c_i^\dagger c_i + \sum_{i,j \in 3QD} (\tilde{t}_{ij} c_i^\dagger c_j + h.c.), \quad (2)$$

where the first term describes the single-level energy ε_i at the i -th QD and the second term corresponds to the electron hopping between QDs. Here, the hopping parameters $\tilde{t}_{12} = t_{12}e^{i\phi/3} = \tilde{t}_{21}^*$, $\tilde{t}_{23} = t_{23}e^{i\phi/3} = \tilde{t}_{32}^*$ and $\tilde{t}_{31} = t_{31}e^{i\phi/3} = \tilde{t}_{13}^*$ include the phase shift $\phi = 2\pi\Phi/(hc/e)$ due to presence of the magnetic flux Φ , hc/e denotes the one electron flux quantum. The spin of electrons is irrelevant in our studies and it is omitted. We consider transport in an open system with the left (L) and right (R) electrode as reservoirs of electrons, each in thermal equilibrium with a given chemical potential μ_α and temperature T_α . The corresponding Hamiltonian is

$$H_{el} = \sum_{k,\alpha \in L,R} \varepsilon_{k,\alpha} c_{k\alpha}^\dagger c_{k\alpha}, \quad (3)$$

where $\varepsilon_{k,\alpha}$ denotes an electron spectrum. The coupling between the 3QD system and the electrodes is given by

$$H_{3QD-el} = \sum_k (t_L c_{kL}^\dagger c_1 + t_R c_{kR}^\dagger c_2 + h.c.) \quad (4)$$

with tunneling from the electrodes given by the hopping parameters t_L and t_R , respectively. The model omits Coulomb interactions, and therefore one can derive analytically all transport characteristics.

B. Calculation of currents

We consider a steady state currents, with the net transport current through the 3QD system $I^{tr} = I_{12} + I_{13}$, expressed as a sum of the bond currents through the upper and the lower branch

$$I_{ij} = \frac{e}{i\hbar} (\tilde{t}_{ij} \langle c_i^\dagger c_j \rangle - \tilde{t}_{ji} \langle c_j^\dagger c_i \rangle). \quad (5)$$

We use the non-equilibrium Green function technique (NEGF), which is described in many textbooks, e.g. see³¹. To determine the currents one calculates the lesser Green functions, $G_{ji}^< \equiv i \langle c_i^\dagger c_j \rangle$, by means of the equation of motion method (EOM). The coupling with the

electrodes is manifested by the lesser Green functions $g_\alpha^< = 2\pi(g_\alpha^r - g_\alpha^a)f_\alpha$, where $g_\alpha^{r,a}$ denotes the retarded (r) and advanced (a) Green function in the α electrode, and $f_\alpha = 1/(\exp[(E - \mu_\alpha)/k_B T_\alpha] + 1)$ is the Fermi distribution function for an electron with an energy E with respect to a chemical potential μ_α and at temperature T_α . For any Green function $G_{ji}^<$ we separate contributions from the left and the right electrode (i.e. we extract the coefficients in front of $g_L^<$ and $g_R^<$), and after some algebra the bond current can be expressed as

$$I_{ij} = -\frac{e}{2\pi\hbar} \int_{-\infty}^{\infty} dE [\mathcal{G}_{ij}^L(E) f_L - \mathcal{G}_{ij}^R(E) f_R], \quad (6)$$

where the dimensionless conductances for the upper and the lower branch are

$$\mathcal{G}_{12}^L = 2\Gamma_L t_{12} \Im[d_{23,31} d_{23,23}^*]/A, \quad (7)$$

$$\mathcal{G}_{12}^R = 2\Gamma_R t_{12} \Im[d_{23,31}^* d_{31,31}^*]/A, \quad (8)$$

$$\mathcal{G}_{13}^L = 2\Gamma_L t_{31} \Im[d_{12,23} d_{23,23}^*]/A, \quad (9)$$

$$\mathcal{G}_{13}^R = 2\Gamma_R t_{31} \Im[d_{12,31} d_{23,31}]/A. \quad (10)$$

Here, we denoted the coefficients: $d_{12,23} = e^{-i\phi} t_{12} t_{23} - t_{31} w_2^r$, $d_{12,31} = t_{12} t_{31} - e^{-i\phi} t_{23} w_1^r$, $d_{23,31} = e^{i\phi} t_{23} t_{31} - t_{12} w_3$, $d_{23,23} = t_{23}^2 - w_2^r w_3$, $d_{31,31} = t_{31}^2 - w_1^r w_3$, and the denominator

$$A = |w_1^r t_{23}^2 + w_2^r t_{31}^2 + w_3 t_{12}^2 - w_1^r w_2^r w_3 - 2t_{12} t_{23} t_{31} \cos \phi|^2, \quad (11)$$

where $w_1^{r,a} = E - \varepsilon_1 - \gamma_L^{r,a}$, $w_2^{r,a} = E - \varepsilon_2 - \gamma_R^{r,a}$, $w_3 = E - \varepsilon_3$, $\Gamma_\alpha = 2\Im[\gamma_\alpha^a] t_\alpha^2$, $\gamma_\alpha^{r,a} = g_\alpha^{r,a} t_\alpha^2$.

Note that the formula (6) includes the transport current due to the bias voltage applied to the electrodes as well as the persistent current induced by the magnetic flux [a term proportional to $\sin \phi$], which can be written as $I_{12} = I_{12}^{tr} - I^\phi$ and $I_{13} = I_{13}^{tr} + I^\phi$. These coefficients are coupled with those (7)-(10):

$$\mathcal{G}_{12}^L = \mathcal{G}_{12} - \mathcal{G}_\phi^L, \quad \mathcal{G}_{12}^R = \mathcal{G}_{12} + \mathcal{G}_\phi^R, \quad (12)$$

$$\mathcal{G}_{13}^L = \mathcal{G}_{13} + \mathcal{G}_\phi^L, \quad \mathcal{G}_{13}^R = \mathcal{G}_{13} - \mathcal{G}_\phi^R. \quad (13)$$

The first part is

$$I_{ij}^{tr} = -\frac{e}{2\pi\hbar} \int_{-\infty}^{\infty} dE (f_L - f_R) \mathcal{G}_{ij}(E), \quad (14)$$

where the bond conductances are

$$\mathcal{G}_{12} = \Gamma_L \Gamma_R t_{12} w_3 [t_{23} t_{31} \cos \phi - t_{12} w_3]/A, \quad (15)$$

$$\mathcal{G}_{13} = \Gamma_L \Gamma_R t_{23} [t_{12} t_{31} w_3 \cos \phi - t_{23} t_{31}^2]/A. \quad (16)$$

The net transport current $I^{tr} = I_{12}^{tr} + I_{13}^{tr}$ and the transmission is given by

$$\begin{aligned} \mathcal{T} &\equiv \mathcal{G}_{12} + \mathcal{G}_{13} \\ &= \Gamma_L \Gamma_R [2t_{12} t_{23} t_{31} w_3 \cos \phi - t_{12}^2 w_3^2 - t_{23}^2 t_{31}^2]/A. \end{aligned} \quad (17)$$

The persistent current is expressed as

$$I^\phi \equiv -\frac{e}{\pi\hbar} \int_{-\infty}^{\infty} dE (\mathcal{G}_\phi^L f_L + \mathcal{G}_\phi^R f_R), \quad (18)$$

where

$$\mathcal{G}_\phi^L = \Gamma_L t_{12} t_{23} t_{31} \sin \phi [2t_2^2 - (w_2^a + w_2^r)w_3]/A, \quad (19)$$

$$\mathcal{G}_\phi^R = \Gamma_R t_{12} t_{23} t_{31} \sin \phi [2t_3^2 - (w_1^a + w_1^r)w_3]/A. \quad (20)$$

Later, in the next section we shall present that the voltage bias can induced the circular current, with the bond conductances \mathcal{G}_{ij} larger than unity or negative.

C. Calculation of current-correlations

Here we consider a single-particle interference effect which takes place in a Mach-Zehnder or Michelson interferometer, but not a Hanbury Brown and Twiss situation with a two-particle interference effect. The current fluctuations are described by the operator $\Delta \hat{I}_{ij}(t) - \langle \hat{I}_{ij}(t) \rangle$, and the current-current correlation function is defined as³²

$$S_{ij,nm}(t, t') \equiv \frac{1}{2} \left[\langle \hat{I}_{ij}(t) \hat{I}_{nm}(t') + \hat{I}_{nm}(t') \hat{I}_{ij}(t) \rangle - 2 \langle \hat{I}_{ij}(t) \rangle \langle \hat{I}_{nm}(t') \rangle \right]. \quad (21)$$

We consider the steady currents, for which the correlation functions can be represented in the frequency domain by their spectral density

$$S_{ij,nm}(\omega) \equiv 2 \int_{-\infty}^{\infty} d\tau e^{i\omega\tau} S_{ij,nm}(\tau). \quad (22)$$

In this work, we shall restrict ourselves to study of the current correlations at the zero-frequency limit $\omega = 0$. Since the net transport current $\hat{I}^{tr} = \hat{I}_{12} + \hat{I}_{13}$, its current correlation function can be expressed as a composition of the correlation functions for the bond currents

$$S_{tr,tr} = S_{12,12} + S_{13,13} + 2S_{12,13}. \quad (23)$$

The correlation functions $S_{ij,in}$ can be derived by means of Wick's theorem³¹ and expressed as

$$\begin{aligned} S_{ij,in} = \frac{e^2}{\pi\hbar} \frac{1}{2} \{ & t_{ij} t_{in} (\langle c_i^\dagger c_j \rangle \langle c_i c_n^\dagger \rangle + \langle c_i^\dagger c_n \rangle \langle c_i c_j^\dagger \rangle) \\ & - t_{ij} t_{ni} (\langle c_i^\dagger c_i \rangle \langle c_n c_j^\dagger \rangle + \langle c_n^\dagger c_j \rangle \langle c_i c_i^\dagger \rangle) \\ & + t_{ji} t_{ni} (\langle c_j^\dagger c_i \rangle \langle c_n c_i^\dagger \rangle + \langle c_n^\dagger c_i \rangle \langle c_j c_i^\dagger \rangle) \\ & - t_{ji} t_{in} (\langle c_i^\dagger c_i \rangle \langle c_j c_n^\dagger \rangle + \langle c_j^\dagger c_n \rangle \langle c_i c_i^\dagger \rangle) \}. \quad (24) \end{aligned}$$

Once again we use the NEGF method. The lesser Green functions, $G_{ji}^< \equiv i \langle c_i^\dagger c_j \rangle$, and the greater Green functions, $G_{ij}^> \equiv -i \langle c_i c_j^\dagger \rangle$, have the same structure, one should only exchange the Green functions in the electrodes: $g_\alpha^< =$

$2\pi(g_\alpha^r - g_\alpha^a)f_\alpha \leftrightarrow g_\alpha^> = -2\pi(g_\alpha^r - g_\alpha^a)(1 - f_\alpha)$. Separating coefficients in front of $f_L(1 - f_L)$, $f_R(1 - f_R)$ and $f_L(1 - f_R) + f_R(1 - f_L)$, after some algebra one can derive a compact formula for any current-current function. The autocorrelation function for the net transport current is given by well know Lesovik's formula^{30,33,34} (see also^{32,35} for a multiterminal and multichannel case)

$$S_{tr,tr} = \frac{e^2}{\pi\hbar} \int_{-\infty}^{\infty} dE \{ \mathcal{T}^2 [f_L(1 - f_L) + f_R(1 - f_R)] + \mathcal{T}(1 - \mathcal{T}) [f_L(1 - f_R) + f_R(1 - f_L)] \}, \quad (25)$$

where \mathcal{T} is the transmission through the 3QD system. For temperature $T_L = T_R = T$ one has $f_L(1 - f_R) + f_R(1 - f_L) = \coth[(\mu_L - \mu_R)/2k_B T](f_L - f_R)$, and thus

$$S_{tr,tr} = 2I^{tr} \coth \left(\frac{eV}{2k_B T} \right) - \frac{e^2}{\pi\hbar} \int_{-\infty}^{\infty} dE \mathcal{T}^2 (f_L - f_R)^2. \quad (26)$$

When the scale of the energy dependence ΔE of the transmission \mathcal{T} is much larger than both the temperature and applied voltage [i.e. $\Delta E \gg eV \gg k_B T$], one can get the well known explicit relation (see Blanter and Buttiker³²)

$$S_{tr,tr} = \frac{e^2}{\pi\hbar} \left[2k_B T \mathcal{T}^2(E_F) + eV \coth \left(\frac{eV}{2k_B T} \right) \mathcal{S}_{tr,tr}^{sh} \right]. \quad (27)$$

The first term is the Nyquist-Johnson noise at the equilibrium and the second term with $\mathcal{S}_{tr,tr}^{sh} = \mathcal{T}(E_F)(1 - \mathcal{T}(E_F))$ corresponds to the shot noise^{30,32,34}.

The correlation functions for the bond currents are calculated from Eq.(24) and expressed as

$$S_{ij,ik} = \frac{e^2}{\pi\hbar} \int_{-\infty}^{\infty} dE \{ \mathcal{S}_{ij,ik}^{sh} [f_L(1 - f_R) + f_R(1 - f_L)] + [\mathcal{G}_{ij}^L \mathcal{G}_{ik}^L f_L(1 - f_L) + \mathcal{G}_{ij}^R \mathcal{G}_{ik}^R f_R(1 - f_R)] \}, \quad (28)$$

where \mathcal{G}_{ij}^α are given by (7)-(10) and the shot noise components are

$$\mathcal{S}_{12,12}^{sh} = \Gamma_L \Gamma_R t_{12}^2 |d_{23,31}^2 - d_{23,23} d_{31,31}^*|^2 / A^2, \quad (29)$$

$$\mathcal{S}_{13,13}^{sh} = \Gamma_L \Gamma_R t_{31}^2 |d_{12,23}^* d_{23,31}^* + d_{12,31} d_{23,23}^*|^2 / A^2, \quad (30)$$

$$\begin{aligned} \mathcal{S}_{12,13}^{sh} = \Gamma_L \Gamma_R t_{12} t_{31} \Re [& (d_{23,31}^2 - d_{23,23} d_{31,31}^*) \\ & \times (d_{12,23}^* d_{23,31}^* + d_{12,31} d_{23,23}^*)] / A^2, \quad (31) \end{aligned}$$

$$\begin{aligned} \mathcal{S}_{tr,tr}^{sh} \equiv \mathcal{S}_{12,12}^{sh} + \mathcal{S}_{13,13}^{sh} + 2\mathcal{S}_{12,13}^{sh} \\ = \Gamma_L \Gamma_R |t_{12} (d_{23,31}^2 - d_{23,23} d_{31,31}^*) \\ + t_{31} (d_{12,23} d_{23,31} + d_{12,31} d_{23,23}^*)|^2 / A^2. \quad (32) \end{aligned}$$

III. BOND CURRENTS AND THEIR CORRELATIONS: DRIVEN CIRCULAR CURRENT IN THE CASE $\Phi = 0$

Let us analyse the bond currents in details, first in the absence of the magnetic flux, $\Phi = 0$, and for a linear response limit $V \rightarrow 0$. Using the derivations from the previous section one can easily calculate the bond conductances and current correlation functions. The results are presented in Fig.2 for an equilateral triangle 3QD system and for various values of the energy level ε_3 at the 3rd QD. The central column corresponds the case with $\varepsilon_1 = \varepsilon_2 = \varepsilon_3 = 0$, when the eigenenergies are given by $E_k = 2t \cos k$, for the wave-vector $k = 0$ and the degenerated state for $k = \pm 2\pi/3$. It is seen in the transmission (black curve), which is equal $\mathcal{T} = 1$ at $E = -2$ and $\mathcal{T} = 0$ at $E = 1$, where the Fano resonance takes place with destructive interference of two electron waves. At low $E < 0$ the incoming wave from the left electrode is split into two branches and the bond conductances are positive, $0 \leq \mathcal{G}_{12}, \mathcal{G}_{13} \leq 1$ (see the blue and green curves in the top panel of Fig.2). The cross-correlation function $\mathcal{S}_{12,13}^{sh}$ (for the currents in both branches) is positive (see the red curve in the bottom panel in Fig.2). Note that at the lowest resonant level all correlation functions $\mathcal{S}_{12,12}^{sh} = \mathcal{S}_{13,13}^{sh} = \mathcal{S}_{12,13}^{sh} = 0$, which means that the currents in both branches are uncorrelated.

For $E > 0$ the conductances, \mathcal{G}_{12} and \mathcal{G}_{13} can be negative and exceed unity (with their maximal absolute values inverse proportional to the coupling Γ_α). It manifests a circular current driven by injected electronic waves to the 3QD system and which can not leave to the drain electrode, therefore they are reflected backwards to the other branch of the ring. The circular current can be characterized by the conductance (see also¹⁶)

$$\mathcal{G}^{dr} \equiv \begin{cases} \mathcal{G}_{12} & \text{for } \mathcal{G}_{12} < 0, \\ -\mathcal{G}_{13} & \text{for } \mathcal{G}_{13} < 0. \end{cases} \quad (33)$$

Here, the superscript "dr" marks the contribution to the circular current driven by the bias voltage, in order to distinguish from the persistent current induced by the flux, which will be analysed later. There is some ambiguity in definition of the circular current. Our definition (33) is similar to that one given by the condition: $\text{sign}[\mathcal{G}_{12}] = -\text{sign}[\mathcal{G}_{13}]$ for the vortex flow used by Jayanavar and Deo³⁶ and by Stefanucci et al.¹⁶ (compare with the other definition³⁷).

For the considered case in Fig.2b, with $\varepsilon_3 = 0$, the circular current is driven counterclockwise for $0 < E < 1$ and it changes its direction to clockwise at the degeneracy point, $E = 1$ (i.e. when \mathcal{G}_{13} becomes negative). All correlation functions are large in the presence of the circular current, their maximum is inverse proportional to Γ_α^2 . The cross-correlation $\mathcal{S}_{12,13}^{sh}$ is large as well but negative, and therefore, this component reduces the transport shot noise, $\mathcal{S}_{tr,tr}^{sh} = \mathcal{S}_{12,12}^{sh} + \mathcal{S}_{13,13}^{sh} + 2\mathcal{S}_{12,13}^{sh}$ to Lesovik's formula $\mathcal{T}(1 - \mathcal{T})$, which reaches zero at the degeneracy point $E = 1$ (see the black curve in Fig.2e). This

situation is similar to multichannel current correlations in transport through a quantum dot connected to magnetic electrodes³⁸, where cross-correlations for currents of different spins usually reduces the total shot noise to a sub-Poissonian noise, with the Fano factor $F < 1$ (however, in the presence of coulomb interactions the cross-correlations can be positive and lead to a super-Poissonian shot noise with $F > 1$).

The plots on the left and right hand side of Fig.2 give more insight into the circular current effect. They are calculated for the dot level $\varepsilon_3 = \mp 2$ - shifted by a gate potential, which breaks the symmetry of the system and removes degeneracy of the states. There are seen 3 resonant levels with $\mathcal{T} = 1$, where two of them are shifted to left/right for $\varepsilon_3 = \mp 2$, but the state at $E = 1$ is unaffected. There is still mirror symmetry, for which one gets three eigenstates, two of them are a linear composition of all local states, but that one at $E = 1$ has the eigenvector $1/\sqrt{2}(c_1^\dagger - c_2^\dagger)|0\rangle$, which is separated for the 3rd QD. Therefore, the bond currents are composition of the currents through all three eigenstates and their contribution depends on E . From these plots one can see that the circular current is driven for $E > \varepsilon_3$, when the cross-correlation $\mathcal{S}_{12,13}^{sh}$ becomes negative. The direction of the current depends on the position of the eigenlevels and their current contributions. For $\varepsilon_3 = -2$ the current circulates clockwise, whereas its direction is counterclockwise for $\varepsilon_3 = 2$.

Here, we assumed the flat band approximation (FBA) for the electronic structure in the electrodes, i.e. the Green functions $g_\alpha^{r,a} = \mp i\pi\rho$, where ρ denotes the density of states. The appendix A presents analytical results for the currents and shot noise in the fully symmetric 3QD system coupled with the semi-infinite chain of atoms. The results are qualitatively similar. However, the FBA is more convenient for the analysis than the system coupled to atomic chains, in particular for the cases with $\varepsilon_3 = \mp 2$ when localized states appear at -2.99 and 2.56, i.e. below/above the energy band of the atomic chain.

The above analysis was performed under the assumption of a smooth energy dependence of the conductance, in the small voltage limit $V \rightarrow 0$ and $T = 0$. However, the conductances exhibit sharp resonant characteristics, in the energy scale $\Delta E \propto \Gamma_\alpha$, and therefore, one can expect that these features will be smoothed out with an increase of voltage bias and temperature. Fig.3 presents the Fano factor $F = \mathcal{S}_{tr,tr}/2eI^{tr}$, which is the ratio of the current correlation function to the net transport current and was calculated numerically from Eq.(17) and (26). At $E = -2$ one can observe the evolution from the coherent regime, from $F = 0$ to $F = 1/2$ in the sequential regime, for $eV \gg \Gamma_\alpha$ or $k_B T \gg \Gamma_\alpha$. Quantum interference plays a crucial role at $E = 1$, leading to the Fano resonance at which the transmission $\mathcal{T} = 0$ and $F = 1$ in the low voltage/temperature regime. An increase of the voltage/temperature results in a small reduction of the Fano factor only.

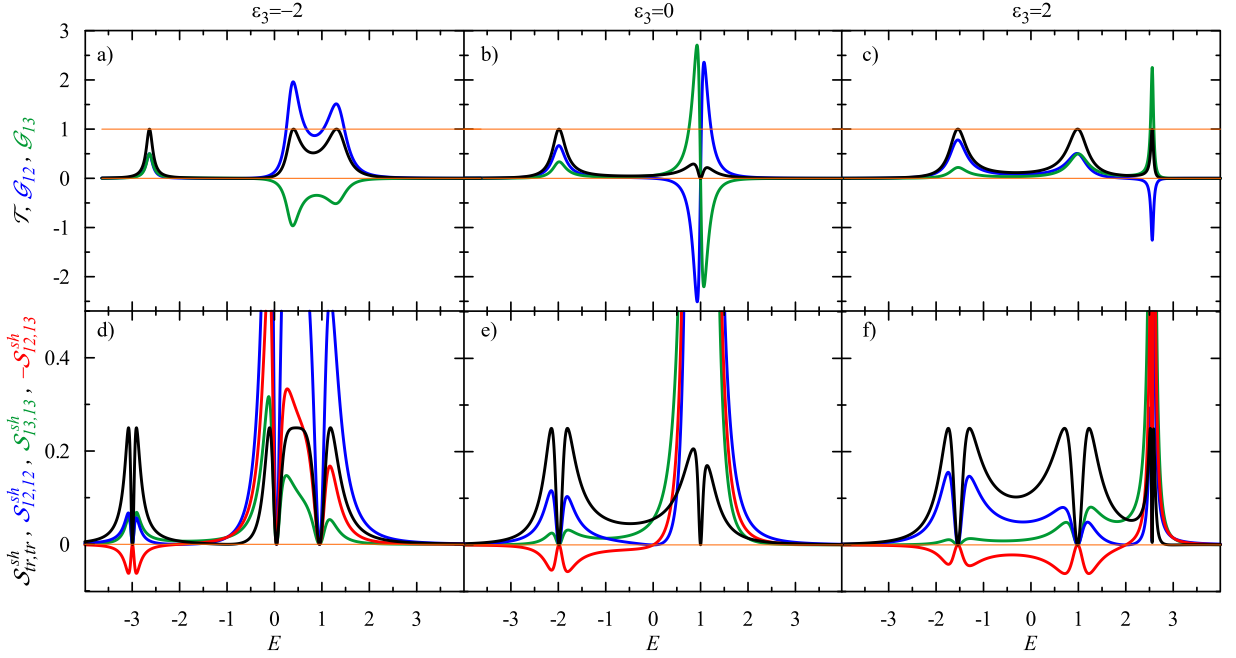


FIG. 2: (Top) Transmission and dimensionless bond conductances: \mathcal{T} - black, \mathcal{G}_{12} - blue, \mathcal{G}_{13} - green, and (Bottom) shot noise: $S_{tr,tr}^{sh}$ - black, $S_{12,12}^{sh}$ - blue, $S_{13,13}^{sh}$ - green, $-S_{12,13}^{sh}$ - red calculated as a function of the electron energy E for the equilateral triangle system of 3QDs (with the interdot hopping $t_{12} = t_{23} = t_{31} = -1$, which is taken as the unity in the paper) in the linear response limit $V \rightarrow 0$. The dot levels: $\varepsilon_1 = \varepsilon_2 = 0$ and $\varepsilon_3 = -2, 0, 2$ - left, center, right column, respectively. The coupling with the electrodes is taken as: $\Gamma_L = \Gamma_R = 0.25$. Note that the cross-correlation function $S_{12,13}^{sh}$ is plotted with the minus sign to show better crossing the zero.

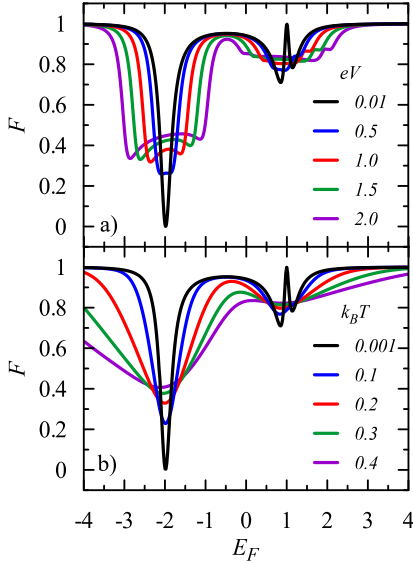


FIG. 3: Fano factor as a function of the Fermi energy E_F for the equilateral triangle 3QDs system ($t_{12} = t_{23} = t_{31} = -1$, $\varepsilon_1 = \varepsilon_2 = \varepsilon_3 = 0$) (top) for various bias voltages $eV = 0.01, 0.5, 1.0, 1.5, 2.0$, at $T = 0$; and (bottom) for various temperatures $k_B T = 0.001, 0.1, 0.2, 0.3, 0.4$, for $V \rightarrow 0$. The coupling to the electrodes is taken $\Gamma_L = \Gamma_R = 0.25$, the chemical potential in the electrodes: $\mu_L = E_F - eV/2$, $\mu_R = E_F + eV/2$.

IV. PERSISTENT CURRENT AND ITS NOISE: THE CASE $V = 0$

The persistent currents and its noise was studied in many papers, e.g. by Büttiker et al.^{39–42}, Semenov and Zaikin^{43–46}, Moskalates⁴⁷, and recently by Komnik and Langhanke⁴⁸ using of full counting statistics (FCS) as well as in 1D Hubbard rings by exact diagonalization by Saha and Maiti⁴⁹ (see also the book by Imry⁵⁰).

Here, we shortly present the results for the persistent current and shot noise in the triangle of 3QDs. Notice that in the considered case the phase coherence length of electrons is assumed to be larger than the ring circumference, $L_\phi \gg L$ ⁵¹. The circular current is given by Eq.(18), which shows that all electrons, up to the chemical potential in the electrodes, are driven by the magnetic flux Φ . Fig.4 exhibits the plots of I^ϕ , derived from Eq.(18), for different couplings with electrodes. In the weak coupling limit $\Gamma \rightarrow 0$ and the perfect ring embedded in the reservoir, the persistent current can be simply expressed as

$$I^\phi = e \sum_k v_k f_k = -\frac{e}{\hbar} \sum_k 2t \sin(k + \phi/3) f_k, \quad (34)$$

where $f_k = 1/(\exp[(E_F - E_k)/k_B T] + 1)$ is the Fermi distribution for the electron with the wave-vector k , the energy $E_k = 2t \cos(k + \phi/3)$, its velocity $v_k = (1/\hbar) \partial E_k / \partial k = (-2t/\hbar) \sin(k + \phi/3)$ and $\phi =$

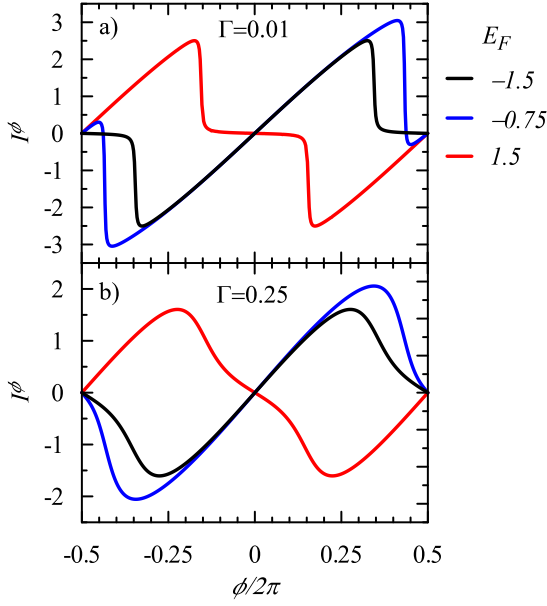


FIG. 4: Persistent current I^ϕ vs. the flux ϕ threaded the equilateral triangle system of 3QDs ($t_{12} = t_{23} = t_{31} = -1$, $\varepsilon_1 = \varepsilon_2 = \varepsilon_3 = 0$). The coupling is taken as $\Gamma_L = \Gamma_R = \Gamma = 0.01$ and 0.25 , the Fermi energies $E_F = -1.5$ (black), -0.75 (blue), 1.5 (red), and $T = 0$.

$2\pi\Phi/(hc/e)$ is the phase shift due to magnetic flux Φ . The sum runs over $k = 2\pi n/(Na)$ for $n = 0, \pm 1$, where $N = 3$ and $a = 1$ is the distance between the sites in the triangle. The current correlator is derived from Eq.(24)

$$S_{\phi,\phi} = \frac{e^2}{h} \sum_k 4t^2 \sin^2(k + \phi/3) f_k (1 - f_k). \quad (35)$$

This result says that fluctuations of the persistent current could occur when the number of electrons in the ring fluctuates, i.e. an electron state moves through the Fermi level and I^ϕ jumps. We show below that the coupling with the electrodes (as a dissipative environment) results in the current fluctuations^{40,41} as well.

At the limit $V \rightarrow 0$ the integrand function of the noise $S_{ij,in}$, Eq.(28), is proportional to $f(E)(1 - f(E))$, which becomes the Dirac delta for $T \rightarrow 0$, and therefore, one can analyze the spectral function $\mathcal{S}_{\phi,\phi} = \mathcal{S}_{12,12} + \mathcal{S}_{13,13} - 2\mathcal{S}_{12,13}$, where its components $\mathcal{S}_{ij,in} = \mathcal{S}_{ij,in}^{sh} + \mathcal{G}_{ij}^L \mathcal{G}_{in}^L + \mathcal{G}_{ij}^R \mathcal{G}_{in}^R$ [see Eq.(7)-(10) and (29)-(31)]. Fig.5, presents the correlation function $\mathcal{S}_{\phi,\phi}$ and its various components for the Fermi energy $E_F = -1.5$ and the strong coupling $\Gamma_L = \Gamma_R = 1$ when fluctuations are large. The noise $\mathcal{S}_{\phi,\phi}$ reaches its maximal value at $\phi \approx \pm 0.36$, i.e. at the jump of I^ϕ (see the black curve in Fig.4a). Notice that the fluctuations of the bond currents $\mathcal{S}_{12,12}$ and $\mathcal{S}_{13,13}$ (the blue and green curve) are different although the average currents are equal. The cross-correlation function $\mathcal{S}_{12,13}$ is positive at $\phi = 0$, but it becomes negative for larger ϕ due to quantum interference, interplay electron waves passing through different states as described in the

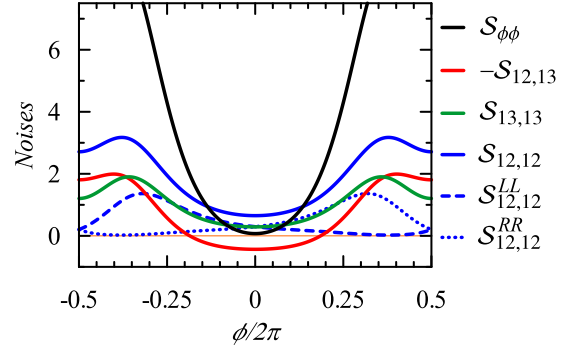


FIG. 5: Flux dependence of spectral function of the persistent current correlator $\mathcal{S}_{\phi,\phi}$ (black) and its components: $\mathcal{S}_{12,12}$ (blue), $\mathcal{S}_{13,13}$ (green), $-\mathcal{S}_{12,13}$ (red), and $\mathcal{S}_{12,12}^L = (\mathcal{G}_{12}^L)^2$ (blue-dashed), $\mathcal{S}_{12,12}^R = (\mathcal{G}_{12}^R)^2$ (blue-dotted), respectively. We assumed the strong coupling: $\Gamma_L = \Gamma_R = 1.0$, $E_F = -1.5$ and $T = 0$.

previous section.

Fig.5 also presents: $(\mathcal{G}_{12}^L)^2$ (blue-dashed curve) and $(\mathcal{G}_{12}^R)^2$ (blue-dotted curve), which correspond to local fluctuations of injected/ejected currents to/from the upper branch on the left and right junction, respectively [see Eq.(28)]. The magnetic flux breaks the symmetry, induces the persistent current and therefore, the local conductances \mathcal{G}_{12}^L and \mathcal{G}_{12}^R are asymmetric.

V. CORRELATION OF PERSISTENT AND TRANSPORT CURRENT, $\Phi \neq 0$ AND $V \neq 0$

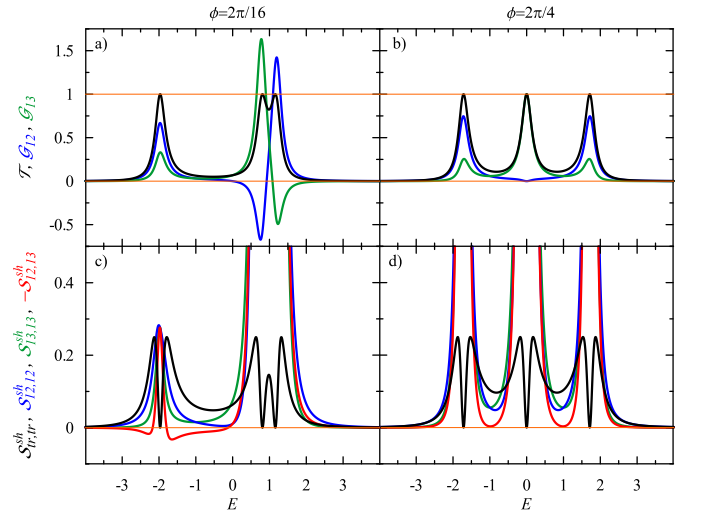


FIG. 6: (Top) Energy dependence of driven conductance \mathcal{G}_{12} (blue), \mathcal{G}_{13} (green) and transmission \mathcal{T} (black) and (Bottom) shot noise $\mathcal{S}_{tr,tr}^{sh}$ (black) with its components: $\mathcal{S}_{12,12}^{sh}$ (blue), $\mathcal{S}_{13,13}^{sh}$ (green), $-\mathcal{S}_{12,13}^{sh}$ (red) for the considered triangular 3QD system threaded by the flux $\phi = 2\pi/16$, $\phi = 2\pi/4$; the coupling $\Gamma_L = \Gamma_R = 0.25$, and $T = 0$. Note that we plot $-\mathcal{S}_{12,13}^{sh}$.

In this chapter we analyze the currents and their correlations in the general case, derived from Eqs.(6),(14),(18) and (28) in the presence of the voltage bias and the magnetic flux. The results for the conductances and the spectral functions of the shot noise are presented in Fig.6. The magnetic flux splits the degenerated levels at $E = 1$ and destroys the Fano resonance. Fig.6a shows that there is not destructive interference already at a small flux $\phi = 2\pi/16$, and the transmission $\mathcal{T} = 1$ for all resonances. One can observe the driven circular current for $E > 0$, with negative \mathcal{G}_{12} and \mathcal{G}_{13} , but their amplitudes are much lower than in the absence of the flux (compare with Fig.2b for $\phi = 0$). For a larger flux, $\phi = 2\pi/4$, there is not the driven component of the circular current (see Fig.6b, where $\mathcal{G}_{12}, \mathcal{G}_{13} \geq 0$). It is also seen that for the state at $E = 0$ the electronic waves pass only through the lower branch of the ring, and the upper branch is blocked (with $\mathcal{G}_{13} = 1$ and $\mathcal{G}_{12} = 0$, respectively).

The lower panel of Fig.6 presents the spectral functions of the shot noise. According Lesovik's formula $\mathcal{S}_{tr,tr}^{sh} = 0$ at the resonant states (due to $\mathcal{T} = 1$). It seems to be similar to the case $\phi = 0$ presented in the lower panel in Fig.2. However, there is a great difference in the components of the shot noise $\mathcal{S}_{ij,in}^{sh}$, indicating on a different nature of transport through these states and a role of quantum interference. Let us focus on the lowest resonant state at $E = -2$ in Fig.6c and compare with that one in Fig.2e in the absence of the flux. In the previous case the currents in both branches were uncorrelated, and $\mathcal{S}_{12,12}^{sh} = \mathcal{S}_{13,13}^{sh} = \mathcal{S}_{12,13}^{sh} = 0$. In the presence of the flux quantum interference becomes relevant and it is seen the shot noise components in Fig.6c. Now, the currents in both branches are correlated; $\mathcal{S}_{12,13}^{sh}$ is negative close to resonance and it fully compensates positive contributions $\mathcal{S}_{12,12}^{sh}$ and $\mathcal{S}_{13,13}^{sh}$ at the resonance. For $\phi = 2\pi/4$ (see Fig.6d), all shot noise components are large, what indicates on a strong quantum interference effect.

Fig.7 presents the Fano factor in the presence of the flux $\phi = 2\pi/16$ and for various bias voltages. Comparing with the results in Fig.3 for $\phi = 0$ one can see how a small flux can destroy quantum interference, and change electron transport. It is particularly seen close to $E = -1$, where the states with the opposite chirality are located. For the case $\phi = 0$ one can observe the Fano resonance with a perfect destructive interference, $\mathcal{T} = 0$ and $F = 1$. With an increase of the flux ϕ the Fano dip disappears, the two states are split and transmission reaches its maximal values $\mathcal{T} = 1$, the Fano factor $F = 0$ when the splitting $\Delta E > \Gamma_\alpha$. A similar effect was seen for the case in Fig.2, where a change of the position of the local level ε_3 removed the state degeneracy and destroyed the Fano resonance.

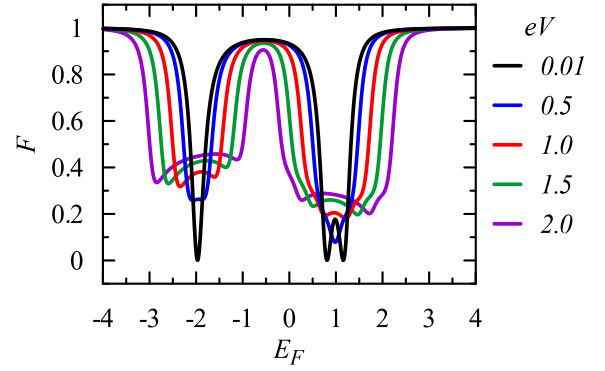


FIG. 7: Fano factor as a function of E_F for the considered 3QD system threaded by the flux $\phi = 2\pi/16$ and for various bias voltages $eV = 0.01, 0.5, 1.0, 1.5, 2.0$. The coupling is taken: $\Gamma_L = \Gamma_R = 0.25$, the chemical potentials $\mu_L = E_F - eV/2$, $\mu_R = E_F + eV/2$, and $T = 0$.

For the strong coupling $\Gamma_L = \Gamma_R = 1$ the intensity of the transport current is comparable to the persistent current and therefore one can expect a significant driven circular current. Fig.8 presents the flux dependence of the total circular current I^c , its driven component I^{dr} as well as the transport current I^{tr} for various voltages. For the considered case $E_F = 0.9$ the driven current circulates counterclockwise and it deforms the flux dependence of the circular current, which become asymmetric.

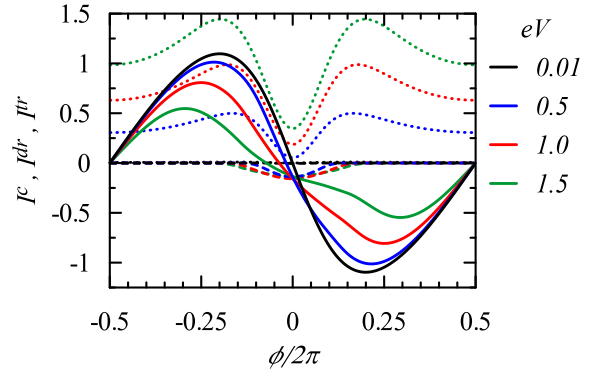


FIG. 8: Circular current $I^c = I^{dr} + I^\phi$ (solid curves), its driven component I^{dr} (dashed curves) and the net transport current I^{tr} (dotted curves) vs ϕ for various bias voltages: $eV = 0.01, 0.5, 1.0$ and 1.5 . We assumed a strong coupling $\Gamma_L = \Gamma_R = 1$, the chemical potentials $\mu_L = E_F - eV/2$, $\mu_R = E_F + eV/2$, $E_F = 0.9$ and $T = 0$.

VI. SUMMARY

We considered influence quantum interference on electron transport and current correlations in the ring of three quantum dots threaded by the magnetic flux. We assumed noninteracting electrons and calculated the bond conductances, the local currents and the current correlation functions, in particular the shot noise, by means of the nonequilibrium Keldysh Green function

technique, taking into account multiple reflections of the electron wave inside the ring. Since we considered elastic scatterings, for which Kirchhoff's current law is fulfilled, the transmission $\mathcal{T} = \mathcal{G}_{12} + \mathcal{G}_{13}$ is a sum of the local bond conductances and the shot noise for the transport current is a composition of the local current correlation functions, $\mathcal{S}_{tr,tr}^{sh} = \mathcal{S}_{12,12}^{sh} + \mathcal{S}_{13,13}^{sh} + 2\mathcal{S}_{12,13}^{sh} = \mathcal{T}(1 - \mathcal{T})$, which gives Lesovik's formula.

In the system with the triangular symmetry the eigenstates $E_0 = -2$ and $E_{\pm} = 1$ (with the wavevector $k = 0$ and $k = \pm 2\pi/3$) play a different role in transport, which is seen in the bond conductances and the shot noise components. An electron wave injected with the energy close to E_0 is perfectly split into both branches of the ring and the current cross-correlation function $\mathcal{S}_{12,13}^{sh}$ is positive. At the resonance E_0 the transmission $\mathcal{T} = 1$ and all correlation functions $\mathcal{S}_{12,12}^{sh} = \mathcal{S}_{13,13}^{sh} = \mathcal{S}_{12,13}^{sh} = 0$, what means that the bond currents are uncorrelated. The magnetic flux changes quantum interference conditions and makes the bond currents correlated; the cross-correlation $\mathcal{S}_{12,13}^{sh}$ becomes negative at the resonance and it fully compensates the positive auto-correlation components $\mathcal{S}_{12,12}^{sh}$, $\mathcal{S}_{13,13}^{sh}$ (with $\mathcal{S}_{tr,tr}^{sh} = 0$).

Quantum interference play a crucial role in transport through the degenerate states at $E_{\pm} = 1$, where one can observe the Fano resonance with destructive interference. In this region the circular current I^{dr} can be driven by the bias voltage. The bond conductances have an opposite sign, their maximal value is inverse proportional to the coupling Γ_{α} with the electrodes and they can be larger than unity. The direction of I^{dr} depends on the bias voltage and the position of the Fermi energy E_F with respect to the degenerate state E_{\pm} . The auto-correlation functions $\mathcal{S}_{12,12}^{sh}$, $\mathcal{S}_{13,13}^{sh}$ are large (inverse proportional to Γ_{α}^2) close to the resonance. The cross-correlator $\mathcal{S}_{12,13}^{sh}$ is negative in the presence of the driven circular current. Our calculations showed that a small magnetic flux, $\phi = 2\pi/16$, can destroy the Fano resonance and two resonance peaks, with $\mathcal{T} = 1$, appear. The driven component I^{dr} is reduced with an increase of ϕ , and it disappears at $\phi = 2\pi/4$. However, quantum interference still plays its role, the bond currents are strongly correlated (with large $\mathcal{S}_{12,12}^{sh}$, $\mathcal{S}_{13,13}^{sh}$ and negative $\mathcal{S}_{12,13}^{sh}$). For the large coupling the driven part I^{dr} can be large and can profoundly modify the total circular current $I^c = I^{dr} + I^{\phi}$.

We also performed calculations of the bond currents and their correlations for rings of a various number of sites, in particular for the benzene ring in the para-, metha- and ortho-connection with the electrodes. The results are qualitatively similar to those presented above for the 3QD ring: quantum interference of travelling waves with the eigenstates of opposite chirality leads to the driven circular currents accompanied by large current fluctuations with a negative cross-correlation component. To observe this effect two conducting branches should be asymmetric. In particular, in the benzene ring the driven circular current appears for the metha and ortho connec-

tion, but it is absent in the para connection when both conducting branches are equivalent (see also⁷).

An open problem is including interactions between electrons into the calculations of the coherent transport and shot noise. Coulomb interactions can be taken into account in the sequential regime⁵², or using the real-time diagrammatic technique⁵³⁻⁵⁵, but in practice one includes only first- and second-order diagrams with respect to the tunnel coupling and a role of QI is diminished. In principle one can treat QI on an equal footing to electron interactions in the framework of the quantum field theory⁵⁶ as it was done for the Anderson single impurity model by means of full counting statistics (FCS) where the average current and all its moments were calculated⁵⁷. However, it is a formidable task even for such simple 3QD model.

Acknowledgments

The research was financed by National Science Centre, Poland project number 2016/21/B/ST3/02160.

Appendix A: Coupling to atomic chain electrodes: Analytic results

The results for the conductances and shot noise may be simplified when we take all hopping integrals equal to t , the same position of the site levels $\varepsilon = 0$ and the symmetric coupling $t_L = t_R = t$ with the electrodes made as a semi-infinite atomic chain. In this case the Green functions in the electrodes are: $g^r = e^{ik}/t$, $g^a = e^{-ik}/t$ and the electron spectrum as $E_k = 2t \cos k$. From Eqs.(7)-(10) one can calculate the dimensionless bond conductances as

$$\mathcal{G}_{12}^L = 2 \sin k [\sin k + \sin 3k - \sin(2k + \phi)] / A, \quad (\text{A1})$$

$$\mathcal{G}_{12}^R = 2 \sin k [\sin k + \sin 3k - \sin(2k - \phi)] / A, \quad (\text{A2})$$

$$\mathcal{G}_{13}^L = 2 \sin k [\sin k - \sin(2k - \phi)] / A, \quad (\text{A3})$$

$$\mathcal{G}_{13}^R = 2 \sin k [\sin k - \sin(2k + \phi)] / A, \quad (\text{A4})$$

where the denominator

$$A = 4 + \cos 2\phi - 2 \cos \phi (3 \cos k - \cos 3k) - \cos 4k. \quad (\text{A5})$$

It is seen an asymmetry with respect to the direction of the magnetic flux (to ϕ) for the conductances \mathcal{G}_{ij}^L and \mathcal{G}_{ij}^R from the left and the right electrode. The transmission \mathcal{T} is expressed as

$$\begin{aligned} \mathcal{T} &\equiv \mathcal{G}_{12}^L + \mathcal{G}_{13}^L = \mathcal{G}_{12}^R + \mathcal{G}_{13}^R = \mathcal{G}_{12} + \mathcal{G}_{13} \\ &= 2 \sin^2 k [1 - 4 \cos k (\cos \phi - \cos k)] / A, \end{aligned} \quad (\text{A6})$$

the driven part of the bond conductances are calculated using Eqs.(15)-(16)

$$\mathcal{G}_{12} = 4 \sin^2 k \cos k (2 \cos k - \cos \phi) / A, \quad (\text{A7})$$

$$\mathcal{G}_{13} = 2 \sin^2 k (1 - 2 \cos \phi \cos k) / A, \quad (\text{A8})$$

$$\mathcal{G}_{\phi}^L = \mathcal{G}_{\phi}^R = 2 \sin \phi \sin k \cos 2k / A, \quad (\text{A9})$$

and from Eqs.(19)-(20) the part induced by the flux

$$\mathcal{G}_{\phi}^L = \mathcal{G}_{\phi}^R = 2 \sin \phi \sin k \cos 2k / A. \quad (\text{A10})$$

It is seen that the conductance \mathcal{G}_{12} becomes negative at $k = \pi/2$, i.e. when the circular current becomes driven.

The shot noise for the bond currents is expressed as

$$\mathcal{S}_{12,12}^{sh} = 4 \sin^2 k |e^{i\phi} (\cos \phi - 2 \cos k) + \cos 2k|^2 / A^2, \quad (\text{A11})$$

$$\mathcal{S}_{13,13}^{sh} = 4 \sin^2 k |\cos k - e^{i\phi}|^2 / A^2, \quad (\text{A12})$$

$$\mathcal{S}_{12,13}^{sh} = -4 \sin^2 k [2 \cos \phi \cos k (\cos \phi - \cos k)^2 + \sin^2 \phi] / A^2, \quad (\text{A13})$$

$$\mathcal{S}_{tr,tr}^{sh} = \mathcal{T}(1 - \mathcal{T}) = 4 \sin^2 k (\cos \phi - \cos k)^2 \times [1 - 4 \cos k (\cos \phi - \cos k)] / A^2. \quad (\text{A14})$$

Notice that the cross-correlation $\mathcal{S}_{12,13}^{sh}$ can be positive or negative in the laminar or the vortex regime, respectively.

-
- ¹ R. A. Webb, S. Washburn, C. P. Umbach, and R. B. Laibowitz, *Physical Review Letters* **54**, 2696 (1985).
 - ² Y. Ji, Y. Chung, D. Sprinzak, M. Heiblum, D. Mahalu, and H. Shtrikman, *Nature* **422**, 415 (2003).
 - ³ D. M. Cardamone, C. A. Stafford, and S. Mazumdar, *Nano Letters* **6**, 2422 (2006).
 - ⁴ G. C. Solomon, D. Q. Andrews, T. Hansen, R. H. Goldsmith, M. R. Wasielewski, R. P. Van Duyne, and M. A. Ratner, *The Journal of Chemical Physics* **129**, 054701 (2008).
 - ⁵ S.-H. Ke, W. Yang, and H. U. Baranger, *Nano Letters* **8**, 3257 (2008), PMID: 18803424.
 - ⁶ A. Donarini, G. Begemann, and M. Grifoni, *Nano Letters* **9**, 2897 (2009).
 - ⁷ D. Rai, O. Hod, and A. Nitzan, *Journal of Physical Chemistry C* **114**, 20583 (2010), arXiv:1006.1729.
 - ⁸ W. Hong, H. Valkenier, G. Mészáros, D. Z. Manrique, A. Mishchenko, A. Putz, P. M. García, C. J. Lambert, J. C. Hummelen, and T. Wandlowski, *Beilstein Journal of Nanotechnology* **2**, 699 (2011).
 - ⁹ C. M. Guédon, H. Valkenier, T. Markussen, K. S. Thygesen, J. C. Hummelen, and S. J. van der Molen, *Nature Nanotechnology* **7**, 305 (2012), arXiv:1108.4357.
 - ¹⁰ C. J. Lambert, *Chemical Society Reviews* **44**, 875 (2015), arXiv:1601.00224.
 - ¹¹ J. Liu, X. Huang, F. Wang, and W. Hong, *Accounts of Chemical Research* **52**, 151 (2019).
 - ¹² S. Nakanishi and M. Tsukada, *Japanese Journal of Applied Physics* **37**, L1400 (1998).
 - ¹³ S. Nakanishi and M. Tsukada, *Physical Review Letters* **87**, 126801 (2001).
 - ¹⁴ I. Daizadeh, J.-x. Guo, and A. Stuchebrukhov, *The Journal of Chemical Physics* **110**, 8865 (1999).
 - ¹⁵ Y. Xue and M. A. Ratner, *Physical Review B* **70**, 1 (2004), arXiv:0405483 [cond-mat].
 - ¹⁶ G. Stefanucci, E. Perfetto, S. Bellucci, and M. Cini, *Physical Review B* **79**, 073406 (2009), arXiv:0903.0557.
 - ¹⁷ D. Rai, O. Hod, and A. Nitzan, *Journal of Physical Chemistry Letters* **2**, 2118 (2011).
 - ¹⁸ D. Rai, O. Hod, and A. Nitzan, *Physical Review B* **85**, 155440 (2012).
 - ¹⁹ H. K. Yadalam and U. Harbola, *Physical Review B* **94**, 1 (2016), arXiv:1606.00638.
 - ²⁰ D. Nozaki and W. G. Schmidt, *Journal of Computational Chemistry* **38**, 1685 (2017).
 - ²¹ M. Patra and S. K. Maiti, *Scientific Reports* **7**, 43343 (2017), arXiv:1607.07273.
 - ²² G. Cabra, A. Jensen, and M. Galperin, *Journal of Chemical Physics* **148**, 1 (2018), arXiv:1803.04462.
 - ²³ M. V. Moskalets, *Europhysics Letters (EPL)* **41**, 189 (1998).
 - ²⁴ V. S. W. Chung, P. Samuelsson, and M. Büttiker, *Physical Review B* **72**, 125320 (2005), arXiv:0505511 [cond-mat].
 - ²⁵ M. Büttiker and P. Samuelsson, *Annalen der Physik* **16**, 751 (2007).
 - ²⁶ S. Pilgram, P. Samuelsson, H. Förster, and M. Büttiker, *Physical Review Letters* **97**, 066801 (2006), arXiv:0512276 [cond-mat].
 - ²⁷ H. Förster, S. Pilgram, and M. Büttiker, *Physical Review B* **72**, 075301 (2005).
 - ²⁸ H. Förster, P. Samuelsson, S. Pilgram, and M. Büttiker, *Physical Review B* **75**, 035340 (2007).
 - ²⁹ C. Bauerle, D. C. Glatli, T. Meunier, F. Portier, P. Roche, P. Roulleau, S. Takada, and X. Waintal, *Reports on*

- Progress in Physics **81**, 056503 (2018), arXiv:1801.07497 .
- ³⁰ G. B. Lesovik, Pis'ma Zh. Eksp. Teor. Fiz. **49**, 513 (1989), [JETP Lett. **49**, 592 (1989)].
 - ³¹ H. Haug and A.-P. Jauho, *Quantum Kinetics in Transport and Optics of Semiconductors* (Springer-Verlag Berlin Heidelberg, 2008).
 - ³² Y. Blanter and M. Büttiker, Physics Reports **336**, 1 (2000), arXiv:9910158 [cond-mat] .
 - ³³ L. S. Levitov and G. B. Lesovik, Pis'ma Zh. Eksp. Teor. Fiz. **55**, 534 (1992), [JETP Lett., 55 (9), 555-559 (1992)].
 - ³⁴ G. B. Lesovik and I. A. Sadovskyy, Physics-Uspokhi **54**, 1007 (2011), arXiv:1408.1966 .
 - ³⁵ T. Martin and R. Landauer, Physical Review B **45**, 1742 (1992).
 - ³⁶ A. M. Jayannavar and P. Singha Deo, Physical Review B **51**, 10175 (1995).
 - ³⁷ One can define the driven current as⁷: $I^{dr} = (I_{12}l_{12} - I_{13}l_{13})/(l_{12} + l_{13})$, where l_{12}, l_{13} denotes the length of the upper and the lower branch. For $I_{13} \rightarrow 0$ one gets a finite circular current, what is an artefact.
 - ³⁸ B. R. Bulka, Physical Review B **62**, 1186 (2000), arXiv:0003418 [cond-mat] .
 - ³⁹ M. Büttiker and C. A. Stafford, Physical Review Letters **76**, 495 (1996).
 - ⁴⁰ P. Cedraschi and M. Büttiker, Journal of Physics: Condensed Matter **10**, 3985 (1998).
 - ⁴¹ P. Cedraschi, V. V. Ponomarenko, and M. Büttiker, Physical Review Letters **84**, 346 (2000).
 - ⁴² P. Cedraschi and M. Büttiker, Annals of Physics **289**, 1 (2000), arXiv:0006440 [cond-mat] .
 - ⁴³ A. G. Semenov and A. D. Zaikin, Journal of Physics: Condensed Matter **22**, 485302 (2010), arXiv:1002.3104 .
 - ⁴⁴ A. G. Semenov and A. D. Zaikin, Physical Review B **84**, 045416 (2011).
 - ⁴⁵ A. G. Semenov and A. D. Zaikin, Physical Review B **88**, 054505 (2013), arXiv:1306.5456 .
 - ⁴⁶ A. G. Semenov and A. D. Zaikin, Physical Review B **94**, 014512 (2016), arXiv:1603.01285 .
 - ⁴⁷ M. Moskalets, Low Temperature Physics **36**, 982 (2010), arXiv:1004.3123v1 .
 - ⁴⁸ A. Komnik and G. W. Langhanke, Physical Review B **90**, 165107 (2014), arXiv:1307.5739 .
 - ⁴⁹ M. Saha and S. K. Maiti, Physica E: Low-Dimensional Systems and Nanostructures **84**, 118 (2016), arXiv:1603.04239 .
 - ⁵⁰ Y. Imry, *Introduction to mesoscopic physics* (Oxford Univ. Press, New York, NY, 1997).
 - ⁵¹ H. F. Cheung, Y. Gefen, E. K. Riedel, and W. H. Shih, Physical Review B **37**, 6050 (1988).
 - ⁵² Y. V. Nazarov and Y. M. Blanter, *Quantum Transport: Introduction to Nanoscience* (Cambridge University Press, 2009).
 - ⁵³ H. Schoeller and G. Schön, Phys. Rev. B **50**, 18436 (1994).
 - ⁵⁴ J. König, J. Schmid, H. Schoeller, and G. Schön, Phys. Rev. B **54**, 16820 (1996).
 - ⁵⁵ A. Thielmann, M. H. Hettler, J. König, and G. Schön, Phys. Rev. Lett. **95**, 146806 (2005).
 - ⁵⁶ A. Kamenev, *Field Theory of Non-Equilibrium Systems* (Cambridge University Press, 2011).
 - ⁵⁷ A. O. Gogolin and A. Komnik, Phys. Rev. B **73**, 195301 (2006).